A NOVEL WAVEGUIDE-TO-MICROSTRIP TRANSITION FOR LOW-COST MILLIMETER-WAVE AND MMIC APPLICATIONS

F.J. Villegas, D.I. Stones and H.A. Hung

TRW Electronic Systems & Technology Division, Redondo Beach, CA 90278

ABSTRACT

A novel waveguide (w/g)-to-microstrip transition has been developed using a new design methodology based on iris coupling. The current design exhibits reduced sensitivity to w/g backshort position and yields a low-cost, hermetically-sealed transition. A 44 GHz-band design on alumina and a 94 GHz-band design on z-cut quartz were implemented, both exhibiting better than 22 dB return loss at their center frequencies with less than 0.3 dB insertion loss, with a greater than 10% bandwidth.

I. INTRODUCTION

In the past, several design methodologies have been proposed in the literature in an effort to introduce an efficient transition from w/g to microstrip. The increased use of low-cost MMIC components such as low-noise and power amplifiers, in both military and commercial systems continues to drive the search for more affordable and package-integrable transitions. This is because the usual method of signal reception and power transmission within a mmW system is via rectangular w/g, due to its relatively low loss and high power handling capability. In order to keep overall package cost to a minimum, it is necessary to design a transition which is mechanically simple and easily integrated into the housing while maintaining an acceptable level of performance.

In the past, transitions based on stepped ridged w/g [1]-[2], antipodal finlines [3], and probe coupling [4]-[5] have been reported in the literature. While these transitions all provide broadband (~10-20% for less than 15 dB return loss) performance with usually less than 0.7 dB insertion loss, the majority of them suffer in their degrees of mechanical complexity. Some of these transitions are sizeable, comprised of several independent pieces that must be assembled in various steps. They may also require: multilevel conductors and substrates, high-tolerance machining of housing components such as w/g steps/tapers, or precise positioning of a backshort. These requirements render some of the designs expensive and difficult to integrate into the package, thus driving the total assembly cost up. In addition, the designs may require a separate w/g window to achieve hermetic sealing of the component.

Figure 1 illustrates a new transition described in this paper.

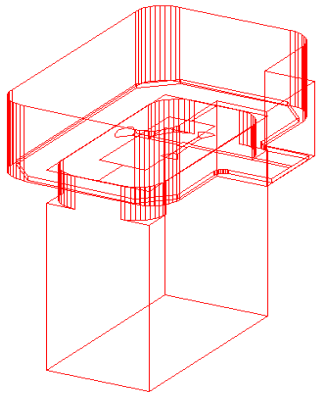

Fig. 1. Illustration of w/g-to-microstrip transition.

Optimal coupling of RF power to and from the w/g is accomplished by making use of a rectangular iris. Impedance matching is accomplished using microstrip circuitry, rendering a very low-profile design, and the printed substrate is eutectically soldered to the housing floor for a hermetic seal. As shown in the figure, a cavity encloses the transition with the exception of the opening for the microstrip. The package ring frame which contains the cavity perimeter is assembled along with the substrate in one step. The cavity cover is also an integral part of the package cover, and can be laser-welded in place, thus making the transition a fully integrated part of the package requiring no special assembly steps. These features render the design very low-cost and readily integrable into typical multi-chip assembly (MCA) packages.

0-7803-4603-6/97/$5.00 (c) IEEE

II. WAVEGUIDE TRANSITION DESIGN

The current transition design, shown in Fig. 2, is based on the concept of a microstrip line coupled to the w/g energy via a slot or iris in the ground plane of the substrate [6]. The microstrip line is situated along the E-plane of the guide, and is terminated in a short coincident with one edge of the iris and connects to the main microstrip line at the other. This ensures a zero voltage condition at the iris edge, and in turn, maximum RF coupling to the radiating line. The dimensions of the cavity enclosing the structure are selected such that

$$\left|\frac{f_0 - f_{res_i}}{f_0}\right| \geq 0.1; i = 1,2 \qquad \text{(EQ 1)}$$

where f_0 is the center operating frequency, and the f_{res_i} are the two closest resonances bounding f_0.

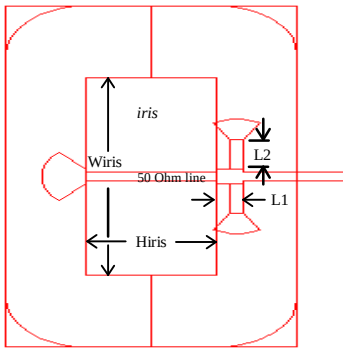

(2a)

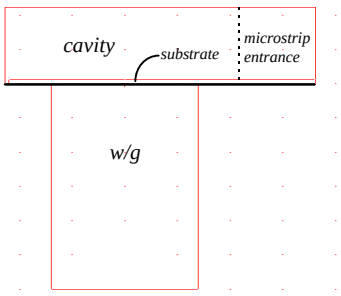

(2b)

Fig. 2. (a) Top view of transition showing matchingnetwork. (b) Side view showing w/g and cavity.

Because of the relative isolation of the cavity from the w/g due to the iris, the exact height of the cavity cover is not crucial to the electrical performance of the transition.

The iris dimensions (H_{iris}, W_{iris}) should be carefully chosen, as this determines the upper bound for the bandwidth of the transition. Essentially, the iris is modeled by a shunt equivalent circuit in which the elements model the storage of susceptive energy caused by non-propagating higher-order modes excited at the discontinuity. These shunt elements can be determined using a variational method such as that described in [7]. In some cases, the iris resonances can be used to broaden the bandwidth of the transition [8]. In the present case, the choice of iris dimensions is accomplished in a different but essentially equivalent manner, using a 3D electromagnetic simulator such as Ansoft's Maxwell Eminence or HP's HFSS. The input impedance referenced to the near edge of the iris is plotted parametrically on the Smith Chart as a family of H_{iris}-curves as a function of W_{iris}, $Z_{in}(W_{iris})$. As illustrated in Fig.3, choosing the curve with the least variation in Z_{in} is equivalent to choosing the iris dimensions that will yield the broadest bandwidth for the matched transition.

Matching the impedance presented by the iris to the microstrip port is accomplished by using two symmetrical, shunt short-circuited lines. The lines begin a short distance L_1 away from the iris edge, as shown in Fig. 2a. Using two symmetrical lines in parallel as opposed to one helps widen the frequency bandwidth; partially due to the higher series reactance seen by the microstrip line. It also tends to yield a more balanced design.

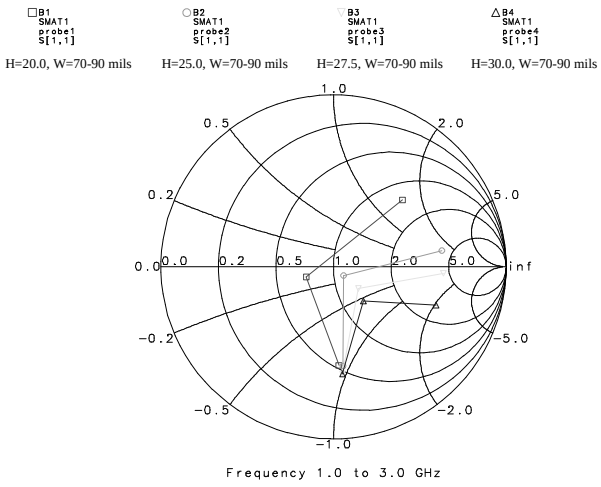

Fig. 3. Smith chart illustrating technique employed to determine optimal iris dimensions. The H=30 mils curve

exhibits the least variation with iris width and hence indicates an overall broader bandwidth.

III. THEORETICAL AND MEASURED RESULTS

Two transitions were assembled and tested based on the aforementioned methodology. One is a Q-band design on 5 mil alumina ($\varepsilon_r = 9.9$), and the other is a W-band design on 5 mil z-cut quartz ($\varepsilon_r = 4.7$). The models were simulated using 3D EM simulators, employing a relatively strict convergence criteria, the details of which are presently omitted. S-parameter measurements of both designs were facilitated by employing two transitions placed in a back-to-back arrangement as shown in Figure 4. The transitions are connected using a 50 Ohm microstrip, 955 mils long for the Q-band fixture and 830 mils for the W-band.

Figure 5 shows the theoretical results for the Q-band transition design. Note that dielectric and planar conductor losses have been accounted for in the model simulation. For a 15 dB return loss, a bandwidth greater than 10% is predicted. The insertion loss throughout the band of interest is ~0.35 dB. Figure 6 shows the Q-band measured data obtained on an automated network analyzer (ANA). The measured results corresponding to one transition can be determined from the back-to-back data. By accounting for the microstrip line and test fixture losses based on separate measurements (1.8 dB/in and 0.2 dB, respectively, at 44 GHz), the return and insertion losses of one transition are calculated. A 10% bandwidth is deduced for a 15 dB return loss, and the insertion loss per transition is found to be less than 0.3 dB. At $f_0 = 44.25$ GHz, a return loss better than 22 dB has been obtained. Another Q-band test fixture was assembled having a cavity height 15 mils smaller, with measured results showing no significant performance degradation. The transitions have been employed in a Q-band power amplifier module. Rigorous testing (over 100 std. Temp. cycles from -40 to 125 degrees centigrade) has proven the hermetic integrity of the module, including the areas surrounding the transitions.

Figure 7 shows the theoretical results for the W-band design, including a microstrip loss of 3.75e07 S/m, and a loss tangent of 2.0e-4. For a 15 dB return loss bandwidth, an insertion loss better than 0.35 dB is predicted. For the W-band design, a lower permittivity substrate was chosen for bandwidth considerations. The higher overall circuit Q in this band may implicitly lead to a narrower response than that at Q-band. Figure 8 shows the W-band back-to-back measured data. A 12% bandwidth with a 15 dB return loss can be deduced.

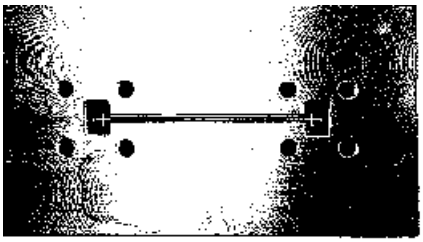

Fig. 4. Top view photo of W-band test fixture sans cover. Note two transitions back-to-back. The Q-band fixture is similar.

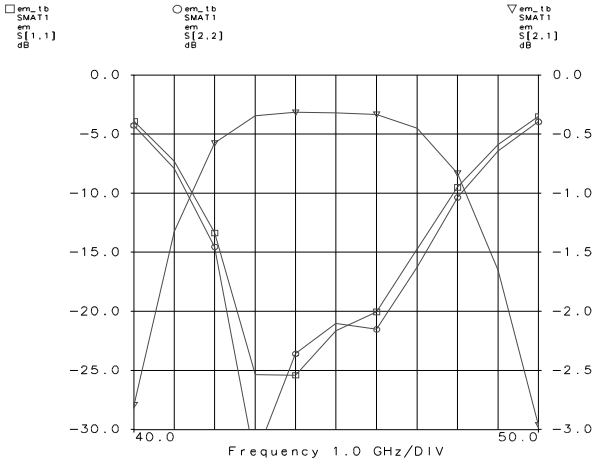

Fig. 5. Theoretical results of Q-band transition. Conductor/dielectric losses are modeled, using a conductivity of 3.8e07 S/m and a loss tangent of 3.0e-4.

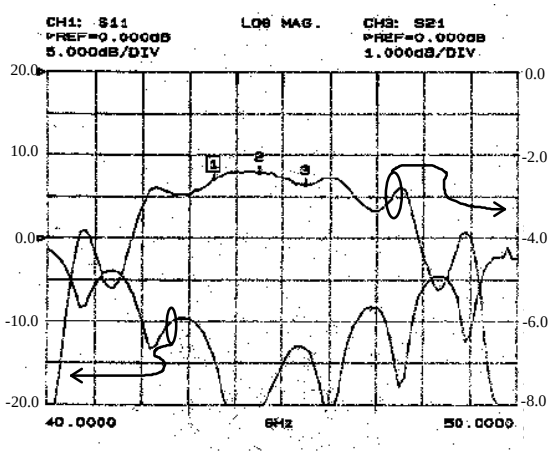

Fig. 6. Measured data of back-to-back Q-band transitions. Material parameters are shown in Fig. 5.

The insertion loss is found to be less than 0.2 dB per transition, using a value of 1.61 dB/in for the microstrip line and test fixture losses at 94 GHz.

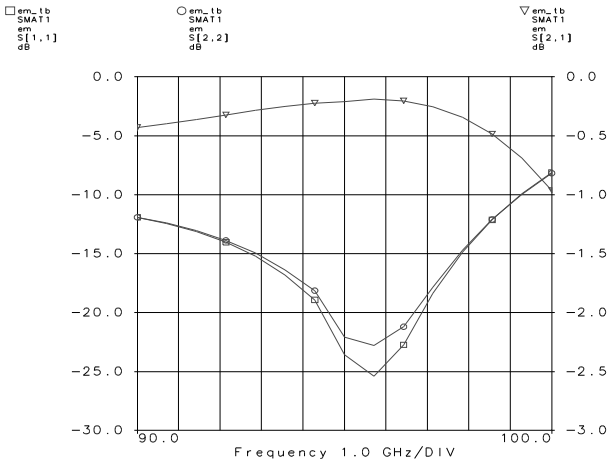

Fig. 7. Theoretical results of W-band transition. Conductor/dielectric losses are modeled.

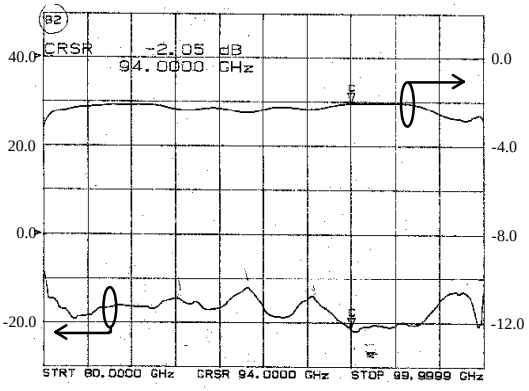

Fig. 8. Measured data of back-to-back W-band transitions.

IV. CONCLUSIONS

A novel w/g-to-microstrip transition has been demonstrated through its implementation in the 44 and 94 GHz-bands. The salient features of the design are: its low manufacturing costs, hermetic sealing of the interface, simple electrical/mechanical design, and relatively broadband performance with low insertion loss. These features provide a transition which can be readily implemented in MMIC-based MCA packages, and as such, has many uses in both military and commercial mmW applications.

V. ACKNOWLEDGEMENTS

This work is supported by the DARPA/ARL/MAFET program. The authors would like to express their gratitude to Ken Park for his valuable assistance in the mechanical design of the transitions.

VI. REFERENCES

[1] S.S. Moochalla, C. An, *"Ridge Waveguide used in Microstrip Transition"*, Microwaves and RF, March 1984.

[2] W. Menzel and A. Klaassen, *"On the Transition from Ridged Waveguide to Microstrip"*, Proc. 19th European Microwave Conf., pp. 1265-1269, 1989.

[3] L.J. Lavedan, *"Design of Waveguide-to-Microstrip Transitions Specially Suited to Millimetre-Wave Applications"*, Electronic Letters, vol. 13, No. 20, pp.604-605, Sept. 1977.

[4] T.Q. Ho and Y.Shih, *"Spectral-Domain Analysis of E-plane Waveguide to Microstrip Transitions"*, IEEE Trans. Microwave Theory and Tech., vol. 37, pp.388-392, Feb. 1989.

[5] D.I. Stones, *"Analysis of a Novel Microstrip-to-Waveguide Transition/Combiner"*, IEEE MTT-S Int'l Symposium Digest, San Diego, Ca, vol. 1, pp.217-220, 1994.

[6] B.N. Das, K.V.S.V.R. Prasad, and S.Rao, *"Excitation of Waveguide by Stripline- and Microstrip-Line-Fed Slots"*, IEEE Trans. Microwave Theory and Tech., vol. 34, pp.321-327, Mar. 1986.

[7] R.E. Collin, *Field Theory of Guided Waves*, McGraw-Hill, New York, ch 8, 1960.

[8] L. Hyvonen and A. Hujanen, *"A Compact MMIC-Compatible Microstrip to Waveguide Transition"*, IEEE MTT-S Int'l Symposium Digest, San Francisco, Ca, vol. 2, pp.875-878, 1996.